E3S Web of Conferences **602**, 01002 (2025) https://doi.org/10.1051/e3sconf/202560201002
ICOME2024

Performance Evaluation of Turbulence Models and Ventilation Strategies in 2D and 3D Simulations: A Comparative Study

Chuhan Zhao [1,*], *Souad* Morsli [2] and *Mohammed* El Ganaoui [3]

[1] University of Lorraine, Master /Science Faculty, France
[2] University of Lorraine, LEM3, ENIM/ Metz, France
[3] University of Lorraine, LERMAB, IUT Henri Poincaré de Longwy, France

Abstract. Recent studies have examined the performance of various turbulence models and ventilation strategies through both 2D and 3D simulations. This research aims to evaluate the effectiveness of turbulence models, such as k-epsilon and k-omega, in simulating airflow and CO_2 distribution under different ventilation conditions. Additionally, the study compares ventilation strategies—including natural, mechanical, and mixed ventilation to assess their impact on energy consumption and indoor air quality. The results indicate that 3D simulations provide a more accurate representation of airflow and CO_2 distribution, which is essential for designing effective ventilation systems. While 2D simulations yield faster results and lower computational costs, they often lack the detail necessary for capturing complex flow dynamics. Among the strategies evaluated, mixed ventilation was found to offer the best balance between energy efficiency and air quality, making it the optimal choice for sustainable building design.

Nomenclature

CO_2: Carbon Dioxide, a common atmospheric gas affecting indoor air quality.
Ppm: Parts Per Million, a unit for measuring gas concentration.
Pa: Pascal, the unit of pressure (N/m²).
$\dot{Q}$: Heat transfer rate, in watts (W).
T: Temperature, measured in Celsius (°C) or Kelvin (K).
ΔP : Pressure difference, in pascals (Pa).
k : Turbulence kinetic energy, in m^2/s^2.
ϵ : Turbulence dissipation rate, in m^2/s^3.
ω : Specific dissipation rate, in 1/s .
P_k: Turbulence production, in m^2/s^3.
R^2: Coefficient of determination, used to assess the fit of regression models.
Re: Reynolds Number, a dimensionless number used to predict flow patterns in fluid dynamics.
U: Flow velocity, in meters per second (m/s).
β : Empirical constant, dimensionless.
α: Empirical constant in k-ω model, dimensionless.
U_j: Mean velocity component in j-direction, in meters per second (m/s).
C1ϵ : Empirical constant in turbulence models.

1. Introduction

Enhancing energy efficiency in buildings is critical for reducing environmental impacts and achieving sustainability goals. However, ventilation systems, while essential for maintaining indoor air quality (IAQ), contribute significantly to a building's overall energy consumption [1-3]. Therefore, optimizing ventilation strategies is crucial to balance energy efficiency with occupant health and comfort.

Indoor air quality directly affects human health and well-being, with pollutants such as carbon dioxide (CO_2) serving as key indicators of ventilation effectiveness and occupancy levels [4-6]. Elevated CO_2 concentrations can lead to adverse health effects, including headaches, fatigue, and decreased cognitive performance [7, 8]. Consequently, controlling indoor CO_2 levels through effective ventilation is essential to ensure a healthy indoor environment.

Ventilation strategies can be broadly categorized into natural, mechanical, and mixed-mode ventilation, each with its own advantages and limitations [9-11]. Natural ventilation utilizes environmental forces such as wind and thermal buoyancy to induce airflow but may result in uneven distribution and is highly dependent on outdoor conditions, including pollution levels [12, 13]. In contrast, mechanical ventilation provides controlled air exchange rates and can effectively manage indoor pollutant levels but is associated with higher energy consumption [1,14]. Mixed-mode ventilation combines natural and mechanical methods to optimize IAQ and energy efficiency, adapting to varying environmental conditions and occupancy demands [15, 16]. Selecting an appropriate ventilation strategy is therefore essential for achieving optimal IAQ while minimizing energy use.

Accurate prediction of airflow patterns and pollutant dispersion within indoor environments is fundamental for designing effective ventilation systems. Computational Fluid Dynamics (CFD) has become an indispensable tool for this purpose [17-20]. The accuracy of CFD simulations largely depends on the

*Corresponding author: chuhan.zhao3@etu.univ-lorraine.fr

choice of turbulence models. The k - ϵ model is widely used due to its robustness and simplicity but may lack precision in predicting near-wall flows [21, 22]. Conversely, the k - ω Shear Stress Transport (SST) model offers improved accuracy for flows with adverse pressure gradients and separation, particularly near walls [2, 24]. Evaluating the performance of these turbulence models is crucial for reliable CFD predictions in ventilation studies [25], which directly impact the design and optimization of ventilation systems.

Moreover, the dimensionality of CFD simulations significantly influences the accuracy of airflow and pollutant dispersion predictions. While two-dimensional (2D) simulations offer reduced computational costs, they may oversimplify complex three-dimensional (3D) airflow dynamics, leading to less accurate results [26]. Three-dimensional simulations, although more computationally intensive, are better suited for capturing vertical stratification and intricate flow interactions critical for detailed IAQ assessments [27]. Understanding the trade-offs between 2D and 3D simulations is vital for efficient and accurate modeling, informing better design decisions in ventilation strategies.

This study aims to perform a comparative evaluation of the k - ϵ and k - ω SST turbulence models within 2D and 3D CFD simulations to assess their effectiveness in predicting airflow patterns and CO_2 distribution under different ventilation strategies. By systematically analyzing natural, mechanical, and mixed ventilation scenarios, we seek to identify optimal modeling approaches and ventilation methods that balance computational efficiency, predictive accuracy, IAQ, and energy performance. The findings are expected to provide valuable insights for the design of efficient and sustainable ventilation systems in building engineering, ultimately supporting the development of healthier and more energy-efficient indoor environments.

2. Methodology

2.1 Model Description:

This study evaluates airflow patterns and CO_2 concentrations under various ventilation strategies using both 2D and 3D simulations. CO_2 concentration serves as a crucial indicator for assessing indoor air quality (IAQ) and pollutant accumulation. By comparing these models, the aim is to evaluate their accuracy and computational demands, particularly in predicting airflow dynamics and pollutant distribution.

The model simulates airflow and CO_2 distribution within a small, rectangular room measuring 2.4 m by 2.1 m, with a height of 2.4 m. Below is a 2D schematic representation of the model, which also serves as a top-down view. External air enters the system from the left side, controlled by a damper, while return air enters the chamber from the right side, 2.1 meters above the floor. Supply air is introduced at 2.1 meters above the ground, located on the right side, adjacent to the return air inlet.

Within the room, there are nine CO_2 generation points arranged in a grid, each positioned 0.5 m apart and located 1.2 m above the ground. Each generation point is represented by a 1 cm diameter pipe, simulating CO_2 emissions from human respiration. The CO_2 flow rate through each pipe is set at 0.0176 m/s, representing the collective emissions of three people working within the room.

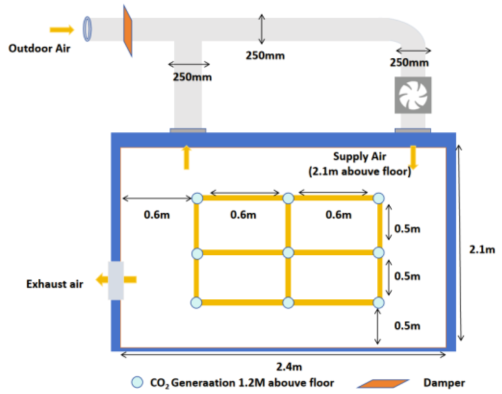

Fig. 1. 2D Schematic Representation of the Ventilation Model Setup.

2D Model: The 2D model simulates airflow but does not account for vertical stratification. We employed the 2D model to compare the k-epsilon and k-omega turbulence models, contrasting the results with the velocity profiles obtained from the 3D simulation.

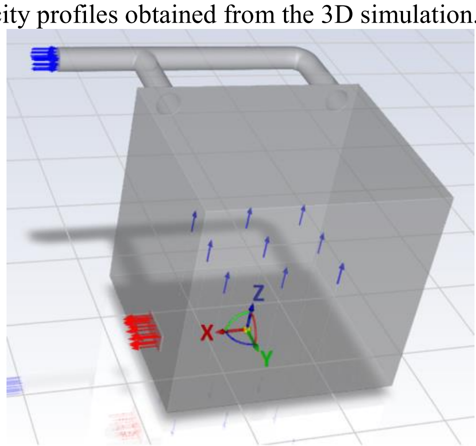

Fig. 2. 3D Model Constructed in Fluent

3D Model: The 3D model captures detailed vertical airflow and stratification, providing a more accurate representation of CO_2 distribution and air age. It serves as the benchmark for evaluating the performance of the 2D model. The model's coordinate axes are shown in Figure 2, with the origin located at the bottom of the CO_2 emission point at the center of the model. The Z-axis is oriented opposite to the direction of gravity, the X-axis runs parallel to the airflow direction towards the exhaust outlet, and the Y-axis is perpendicular to the airflow direction at the exhaust outlet.

To facilitate comparison between the 2D and 3D models, the fan in the 2D model is configured as a constant pressure line segment, while the fan in the 3D model is represented as a constant pressure circular surface, both with a length or diameter of 250 mm.

The study compares three ventilation strategies: natural, mechanical, and mixed ventilation. For each strategy, simulations are conducted to assess:

CO_2 Distribution: Illustrated using contour plots

Average CO_2 Concentration: Focusing on how each strategy maintains indoor air quality (IAQ).

Efficient ventilation ensures regular air replacement and prevents pollutant buildup. By evaluating CO_2 distribution and concentration under different ventilation strategies, the study identifies the most effective method for balancing IAQ and energy efficiency.

2.2 Turbulence Models:

Two turbulence models were employed in all simulations to capture airflow dynamics: the k-ε realizable EWF model and the k-ω SST model.

The k-ε realizable model is widely used for high-Reynolds-number flows, delivering robust results for turbulent airflows. Its transport equations for turbulent kinetic energy (k) and dissipation rate (ϵ) are as follows:

$$\frac{\partial k}{\partial t} + U_j \frac{\partial k}{\partial x_j} = P_k - \epsilon \qquad (1)$$

$$\frac{\partial \epsilon}{\partial t} + U_j \frac{\partial \epsilon}{\partial x_j} = C_1 \frac{\epsilon}{k} P_k - C_1 \epsilon^2 \qquad (2)$$

The k-ω model is particularly well-suited for capturing near-wall effects, especially in low-Reynolds-number flows. Its governing equations consist of the transport equations for turbulent kinetic energy (k) and specific dissipation rate (ω):

$$\frac{\partial k}{\partial t} + U_j \frac{\partial k}{\partial x_j} = P_k - \beta^* k \omega \qquad (3)$$

$$\frac{\partial \omega}{\partial t} + U_j \frac{\partial \omega}{\partial x_j} = \alpha \frac{\omega}{k} P_k - \beta \omega^2 \qquad (4)$$

These models are used to simulate airflow and calculate air age, which indicates the amount of time air spends in different regions of the room. This metric reflects the efficiency of the ventilation system.

2.3 Computational Tools and Setup:

All simulations were conducted using ANSYS Fluent [28], incorporating the Boussinesq approximation to account for buoyancy effects due to temperature differences. Air was modelled as a compressible fluid under steady-state conditions, with the fluid properties summarized in the table below:

Table 1. Fluid Properties for Air and Carbon Dioxide at 300 K

Property	**T_0 (K)**	**ρ_0 (Kg m^{-3})**	**C_{p0} (J Kg^{-1} K^{-3})**	**λ_0 (Wm^{-1} K^{-1})**	**μ_0 (Kg m^{-1} s^{-1})**	**β_T (K^{-1})**	**Pr**
Air	300	1.225	1006.43	0.0242	1.7894 10^{-5}	0.00341	0.71
Carbon Dioxide	300	1.7878	840.37	0.0145	1.37 10^{-5}	0.00341	0.71

After comparing different types of meshes, we ultimately decided to use a quadrilateral mesh in the room, with a maximum cell length of 3 cm. Near the walls, as well as at the inlet and outlet, smaller cells with a side length of 1 cm were used, featuring 10 inflation layers with an expansion factor of 1.1 to accurately capture airflow patterns. The total number of nodes in the mesh for 3D was 2,728,473 and 2D was 152,231.

Key boundary conditions include:

Inlet: A pressure inlet condition was applied at the 250 mm diameter duct for all models.

Outlet: A pressure outlet was positioned at the opposite end of the room to simulate air exhaust.

Walls: In the 3D model, no-slip boundary conditions were applied to the walls of both the room and the duct, with a temperature set to 300 K.

3. Results and Discussion

3.1 Comparison of Turbulence Models (k-epsilon EWF vs. k-omega SST)

In this section, we compare two widely used turbulence models: k-epsilon EWF and k-omega SST. Both models have their strengths and limitations, particularly when simulating airflow near walls or in scenarios involving complex flow dynamics.

The k-epsilon model is recognized for its robustness in simulating fully turbulent flows, especially in free-stream regions. However, it often struggles with precision near walls, where flow separation or strong gradients occur. In contrast, the k-omega SST model is specifically designed to handle boundary layers more effectively, providing better accuracy in these areas. This characteristic makes the k-omega SST model a suitable choice for scenarios involving wall-bounded flows and significant shear forces.

To compare these models, we conducted a series of simulations. The air velocity at the inlet was monitored as the damper rotated from a vertical to a horizontal position over a 180-second period at a rate of 0.5° per second. The results presented in Figure 3, highlight the performance differences between the two models. The k-omega model consistently provided smoother and more stable results, particularly between 51° and 53°, where the k-epsilon model exhibited instability.

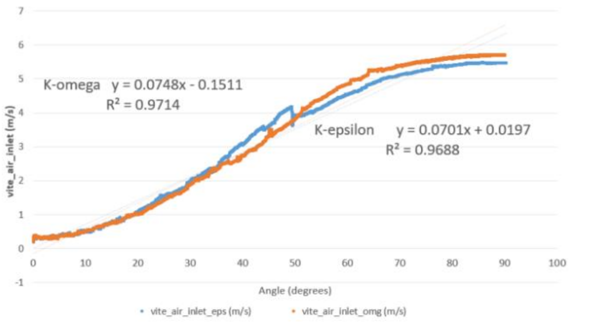

Fig. 3. Comparison of K-epsilon and K-omega Models on Air Inlet Velocity

We observed that, while both models exhibited similar trends in airflow velocity for most of the simulation, the k-epsilon model displayed noticeable deviations at certain critical angles, particularly from 0° to 51°, as illustrated in Figure 4. These deviations are likely attributed to the model's approach to handling boundary layer turbulence, where the k-omega model demonstrated greater stability.

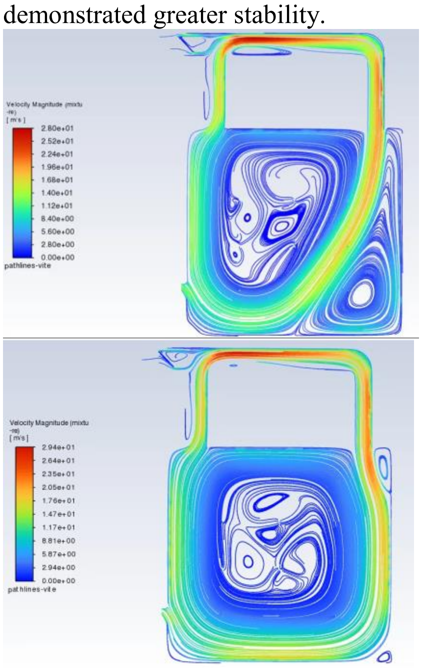

Fig. 4. Simulation results of the K-epsilon model (top) and the K-omega model (bottom) at a damper angle of 51°.

Overall, the k-omega model exhibited greater accuracy and stability in capturing complex flow dynamics near walls. This superiority is particularly evident in scenarios involving minor perturbations or significant shear forces. In contrast, while the k-epsilon model is generally reliable, it struggled to maintain accuracy in these challenging regions.

This comparison confirms that for simulations involving boundary layer effects or wall interactions, the k-omega SST model provides a more accurate representation of the physical phenomena. It is especially beneficial in transient scenarios where the flow experiences rapid changes or disturbances, as demonstrated in our simulations.

3.2 Comparison of 2D, and 3D Models

In this study, we compared airflow dynamics in a simulated room using both 2D and 3D models with varying fan pressures to evaluate the accuracy of wall-bounded flows, velocity fields, and computational efficiency.

The 2D model with a fan pressure of 500 Pa significantly overestimated wall velocities due to the absence of the third dimension, where the vertical axis is assumed to be infinitely extended. In contrast, the 3D model at the same fan pressure provided a more accurate distribution of wall velocities, demonstrating that 2D simulations are inadequate for handling large-scale models.

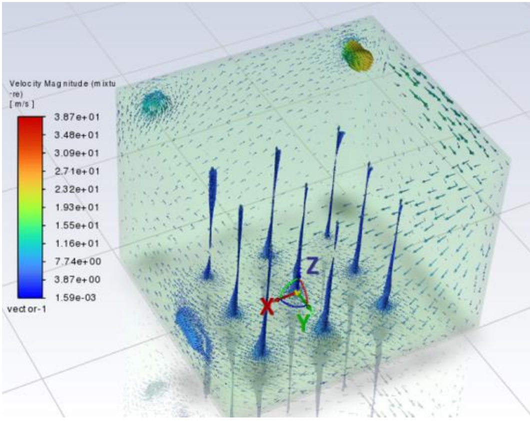

Fig. 5. 3D Room Velocity Vector at Fan Pressure 500 Pa, Damper 51°

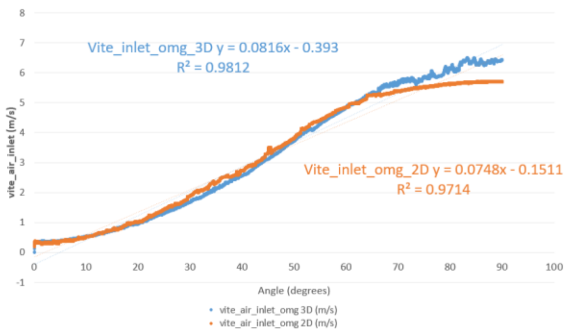

Fig. 6. 3D Room Velocity Vector at Fan Pressure 500 Pa, Damper 51°

At a fan pressure of 500 Pa, we observed good consistency in the weighted average velocity between the 2D and 3D models (Figure 6). Comparing the 2D model (Figure 4) and the 3D model (Figure 5), we found that the 3D model provided more realistic wall velocities. It offered a detailed representation of flow dynamics, capturing the complex interactions near the walls and within the overall room geometry. While the 2D model delivered faster results with lower computational requirements, it lacked the accuracy needed for scenarios involving detailed wall-bounded flow and vertical stratification of air.

3.3 Natural, Mechanical, and Mixed Ventilation Comparisons

In this study, we simulated airflow dynamics and CO_2 distribution under three different ventilation scenarios: natural ventilation, mechanical ventilation, and mixed ventilation. The objective was to assess how these strategies affect the distribution of CO_2 within the room, with a particular focus on identifying areas where CO_2 may stagnate. Below, we summarize the results for each scenario.

3.3.1 Natural Ventilation:

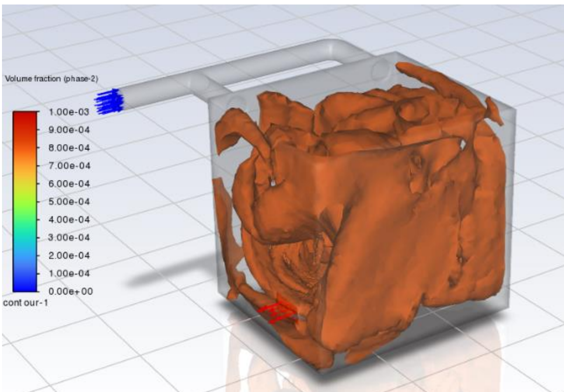

Fig. 7. CO_2 Iso-Surface for 800 PPM in the Natural Ventilation Scenario

Under natural ventilation conditions, with an inlet pressure of 5 Pa and no active fan support, the room exhibited an overall average CO_2 concentration of 1055 PPM (Figure 7). The overall CO_2 concentration in the room was relatively high, and significant accumulation was observed in the central regions as well as at heights below 1.7 meters (Figure 8). This indicates that natural ventilation is insufficient to maintain overall air quality, and it is less effective in ensuring a uniform distribution of carbon dioxide, especially in areas distant from the ventilation openings. Over time, this could pose a risk to indoor air quality, as CO_2 levels may rise in regions with weaker air circulation.

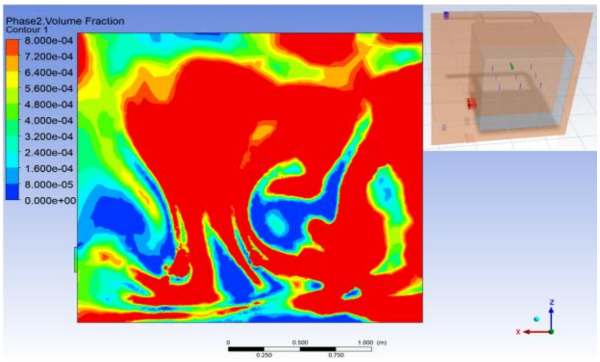

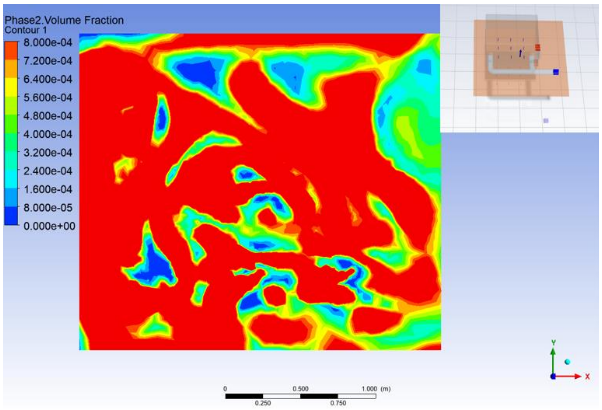

Fig. 8. Contour plots of CO_2 concentration at Y=0.4 m（Top） and Z=1.3 m (Bottom) for Natural Ventilation

The green and red areas in the Phase 2 volume fraction maps indicate elevated concentrations of CO_2, particularly in the central zones of the room. These contour plots illustrate CO_2 concentration at various heights, revealing that higher levels are predominantly found near the lower and central regions. The red regions specifically mark areas of the highest concentration, emphasizing the need for improved airflow in these critical zones.

3.3.2 Mechanical Ventilation:

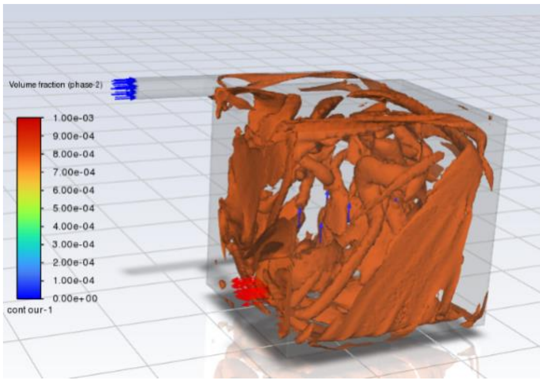

Fig. 9. CO_2 Iso-Surface for 800 PPM in the Mechanical Ventilation.

In the mechanical ventilation scenario, we established the inlet pressure at 0 Pa and simulated a fan that supplied an additional pressure of 30 Pa. This configuration resulted in a significantly lower average CO_2 concentration of 501 PPM (Figure 9).

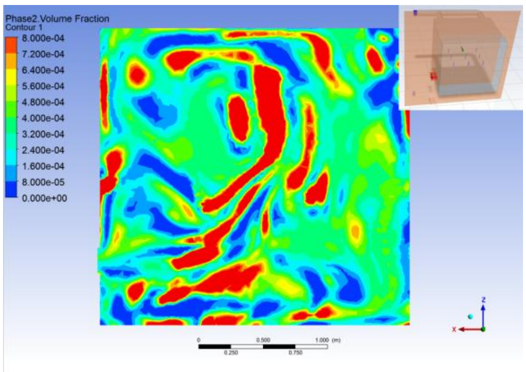

Fig. 10. Contour plots of CO_2 concentration at Y=0.4 m for Mechanical Ventilation

More importantly, the CO_2 distribution was notably more uniform throughout the room (Figure 10), with no significant areas of stagnation. Mechanical ventilation effectively circulated the air, thereby preventing CO_2 buildup in specific regions.

3.3.3 Mixed Ventilation:

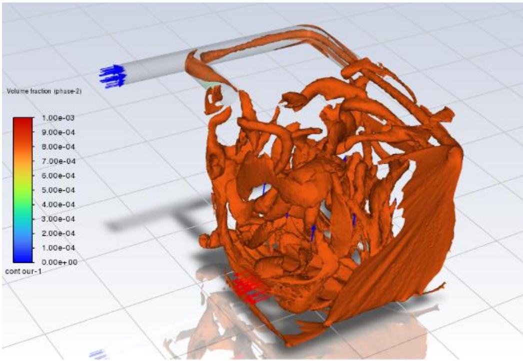

Fig. 11. CO_2 Iso-Surface for 800 PPM in the Mixed Ventilation.

In the mixed ventilation scenario, where the inlet pressure remained at 5 Pa, but a fan applied 30 Pa of pressure, the average CO_2 concentration further dropped to 397 PPM (Figure 11). Like the mechanical ventilation case, CO_2 distribution remained highly uniform, with no noticeable areas of stagnation (Figure 12).

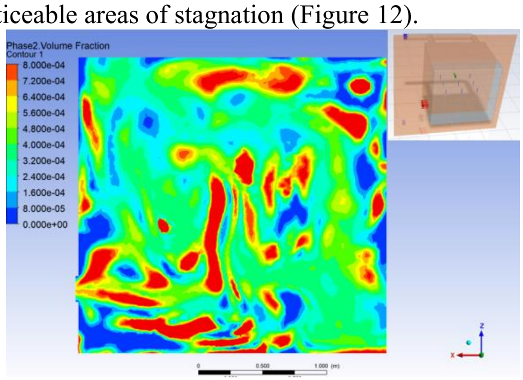

Fig. 12. Contour plots of CO_2 concentration at Y=0.4 m for Mixed Ventilation

The mixed ventilation strategy demonstrated a slight enhancement over mechanical ventilation, both in terms of average CO_2 levels and distribution efficiency.

4. Conclusion

Comparing the three ventilation methods reveals significant limitations of natural ventilation in achieving acceptable average CO_2 concentration levels. Uneven airflow hinders its effectiveness, particularly in areas with poor circulation, leading to considerable CO_2 accumulation in the central and lower parts of the room. In contrast, mechanical and mixed ventilation methods maintain lower overall CO_2 concentrations while ensuring more uniform air distribution, effectively preventing high-concentration zones.

These findings indicate that natural ventilation fails to meet essential air renewal requirements, while mechanical and mixed strategies are more effective in sustaining optimal indoor air quality over time. The figure below (Figure 13) visually illustrates the average CO_2 concentrations across the three scenarios, further demonstrating that mixed and mechanical ventilation outperform natural ventilation in maintaining low CO_2 levels. Figure 14 also verifies this conclusion through the analysis of inlet air velocity.

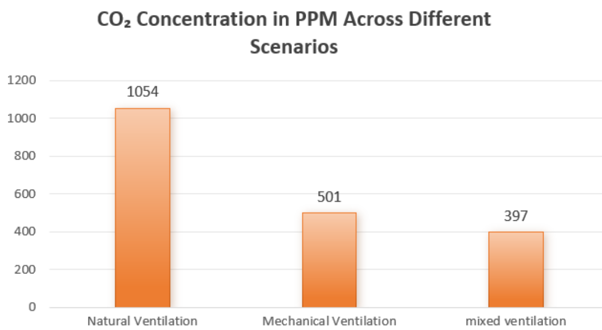

Fig. 13. CO_2 Concentration Comparison across Different Ventilation Scenarios: Natural Ventilation, Mechanical Ventilation, and Mixed Ventilation.

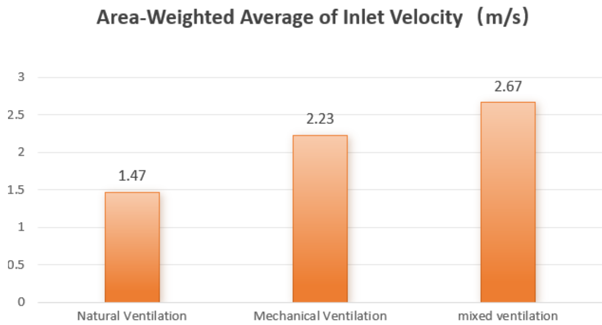

Fig. 14. Area-Weighted Average of Inlet Velocity

Although natural ventilation can reduce CO_2 levels to some extent, it is far less effective than mechanical and mixed systems in providing even air distribution throughout the room. This uneven distribution can create stagnant areas, potentially compromising indoor air quality over time. In contrast, the mixed ventilation system strikes an optimal balance between CO_2 reduction and uniform air distribution, making it the most efficient choice for ensuring high indoor air quality.

This approach not only enhances occupant comfort but also fosters a healthier indoor environment, which is essential for long-term well-being. Furthermore, by effectively managing air quality, mixed ventilation can contribute to improved productivity and overall quality of life for occupants. Thus, integrating mixed ventilation strategies into building design is a prudent choice for creating sustainable and healthy living spaces.

REFERENCES

1. Li, Y. L., Han, M. Y., Liu, S. Y., & Chen, G. Q. (2019). Energy consumption and greenhouse gas emissions by buildings: A multi-scale perspective. *Building and Environment*, 151, 240-250.
2. Geng, Y., Chen, W., Liu, Z., Chiu, A. S., Han, W., Liu, Z., ... & Cui, X. (2017). A bibliometric review: Energy consumption and greenhouse gas emissions in the residential sector. *Journal of Cleaner Production*, 159, 301-316.
3. Mills, E. (2011). Building commissioning: A golden opportunity for reducing energy costs and greenhouse gas emissions in the United States. *Energy Efficiency*, 4, 145-173.
4. Jones, A. P. (1999). Indoor air quality and health. *Atmospheric Environment*, 33(28), 4535-4564.
5. Wolkoff, P. (2018). Indoor air humidity, air quality, and health—An overview. *International Journal of Hygiene and Environmental Health*, 221(3), 376-390.
6. Allen, J. G., MacNaughton, P., Laurent, J. G. C., Flanigan, S. S., Eitland, E. S., & Spengler, J. D. (2015). Green buildings and health. *Current Environmental Health Reports*, 2, 250-258.
7. Satish, U., Mendell, M. J., Shekhar, K., Hotchi, T., Sullivan, D., Streufert, S., & Fisk, W. J. (2012). Is CO_2 an indoor pollutant? Direct effects of low-to-moderate CO_2 concentrations on human decision-making performance. *Environmental Health Perspectives*, 120(12), 1671-1677.
8. Persily, A. K., & de Jonge, L. (2017). Carbon dioxide generation rates for building occupants. *Indoor Air*, 27(5), 868-879.
9. Chenari, B., Carrilho, J. D., & Da Silva, M. G. (2016). Towards sustainable, energy-efficient and healthy ventilation strategies in buildings: A review. *Renewable and Sustainable Energy Reviews*, 59, 1426-1447.
10. Su, W., Ai, Z., Liu, J., Yang, B., & Wang, F. (2023). Maintaining an acceptable indoor air quality of spaces by intentional natural ventilation or intermittent mechanical ventilation with minimum energy use. *Applied Energy*, 348, 121504.
11. Brager, G., Alspach, P., & Nall, D. H. (2011). Natural vs. mechanical ventilation and cooling. *ASHRAE Transactions*, 117(2), 311-323.
12. Shrestha, P. M., Humphrey, J. L., Carlton, E. J., Adgate, J. L., Barton, K. E., Root, E. D., & Miller, S. L. (2019). Impact of outdoor air pollution on indoor air quality in low-income homes during wildfire seasons. *International Journal of Environmental Research and Public Health*, 16(19), 3535.
13. Spiru, P., & Simona, P. L. (2017). A review on interactions between energy performance of the buildings, outdoor air pollution and the indoor air quality. *Energy Procedia*, 128, 179-186.
14. Kwon, S., Lee, K., & Jo, J. H. (2021). Energy-saving potential of mechanical ventilation with heat recovery in residential buildings considering occupant behavior. *Sustainable Cities and Society*, 70, 102861.
15. Morsli, S., Bennacer, R., El Ganaoui, M., Ramenah, H., & Carmasol, A. (2019). Some flow patterns within ventilation strategy coupled to energy efficiency. *The European Physical Journal Applied Physics*, 88(1), 10902.
16. Ozarisoy, B., & Altan, H. (2023). Energy policy design in the Eastern Mediterranean basin: A roadmap to energy efficiency. Routledge.
17. Krajčík, M., Simone, A., & Olesen, B. W. (2012). CFD modeling of airflow and heat transfer in a room heated by warm air. *Energy and Buildings*, 55, 476-484.
18. Morsli, S., Ramenah, H., El Ganaoui, M., & Bennacer, R. (2018). Effect of aligned and misaligned ventilation opening affecting energy demand and air quality in buildings. The European Physical Journal Applied Physics, 83(1), 10901.
19. van Hooff, T., & Blocken, B. (2015). Coupled urban wind flow and indoor natural ventilation modelling on a high-resolution grid: A case study for the Amsterdam ArenA stadium. *Environmental Modelling & Software*, 66, 1-16.
20. Morsli, S., Boussoufi, M., Sabeur, A., El Ganaoui, M., & Bennacer, R. (2018). Small to large scale mixed turbulent convection: Buildings application. *International Journal of Numerical Methods for Heat & Fluid Flow*, 28(1), 188-205.
21. Launder, B. E., & Spalding, D. B. (1974). The numerical computation of turbulent flows. *Computer Methods in Applied Mechanics and Engineering*, 3(2), 269-289.
22. Hanjalić, K., & Launder, B. E. (2011). Modelling turbulence in engineering and the environment: Second-moment routes to closure. Cambridge University Press.
23. Menter, F. R. (1994). Two-equation eddy-viscosity turbulence models for engineering applications. *AIAA Journal*, 32(8), 1598-1605.
24. Abd Halim, M. A., Mohd, N. N., Nasir, M. M., & Dahalan, M. N. (2018). The evaluation of k - ϵ and k - ω turbulence models in modelling flows and performance of s-shaped diffuser. *International Journal of Automotive and Mechanical Engineering*, 15(2), 5290-5306.
25. Krajčík, M., Simone, A., & Olesen, B. W. (2012). CFD modeling of airflow and heat transfer in a room heated by warm air. *Energy and Buildings*, 55, 476-484.
26. Lemaire, A. D., Bricteux, L., & Dehghan, A. (2013). Limitations of two-dimensional simulations for building airflow predictions. *Building and Environment*, 64, 122-132.

27. Feng, G., Chen, X., & Li, X. (2021). Comparative study of 2D and 3D CFD simulations for predicting airflow and contaminant dispersion in an aircraft cabin. *Building and Environment*, 190, 107530.
28. Fluent Inc. (2006). *FLUENT 6.3.26 User's guide*. Fluent Inc.